Aberrant Middle Prefrontal-Motor Cortex Connectivity Mediates Motor Inhibitory Biomarker in Schizophrenia

Supplementary Information

Supplemental Methods and Materials

TMS and electromyography procedure

A figure-of-eight coil (70 mm diameter) with Magstim 200 BiStim stimulators (Magstim Co., Whitland, UK) was utilized to deliver the stimulations. The coil was held pointing backward and rotated 45° away from the midline (1-3). Each subject's structural images were used for precise positioning of the coil through Brainsight™ Navigation system (Rogue Research Inc, Montreal, Canada). The stimulus target was left motor cortex (M1) where TMS induced the maximum response from right first dorsal interosseous muscle using surface electromyography (EMG) with NeuroScan synamp^2 amplifier (Charlotte, NC) amplified (gain of 10) and sampled at 1000 Hz (4, 5). Peak-to-peak amplitude of the motor-evoked potentials (MEP) was measured. The EMG root mean squared (RMS) value from 50 to 5ms prior to TMS pulse was verified to ensure appropriate resting levels for each trial.

Resting motor threshold (RMT) was defined as the minimum intensity needed to elicit a MEP of>50μV in at least 5 out of 10 consecutive stimuli (5). Paired-pulse TMS (ppTMS) with 1 and 3 ms ISIs (6, 7) were used to represent short-interval intracortical inhibition (SICI). For each SICI trial, a subthreshold conditioning stimulus (80% RMT) was followed by a suprathreshold stimulation (120% RMT, TS). Single 120% RMT stimuli were delivered as a control condition (TS alone). There were 12 trials for TS alone and SICI (6 trials for 1 and 3 ms ISIs, respectively)

in one session. The intertrial intervals were 4 seconds or longer. Participants were evaluated in two sessions about 4 weeks apart to ensure reproducibility of the SICI effects. SICI was reliable and the two sessions did not show significant differences in any ISIs or TS alone (all paired *t*-test $p>0.05$). We then merged the two sessions to represent SICI. Therefore, there were 24 trials for SICI and TS alone, respectively. SICI was defined as the ratio between responses of ppTMS and TS alone. Ratios less than 1 indicate inhibition and the smaller the ratio (smaller SICI values), the stronger the cortical inhibition and less deficit in this function.

Resting state data preprocessing

Pre-processing steps were carried out using Analysis of Functional NeuroImages (AFNI) (8) software (Version 16.3.17). Scan from each participant underwent standard preprocessing included standard procedures for slice-timing correction, spatial smoothing of 4mm (with a full width at half maximum Gaussian kernel), linear detrending, and removal of nuisance signals related to head motion, white matter and cerebral spinal fluid (CSF). Resting state functional data were co-registered to the T1 anatomical images, and then transformed to standard space. The spatial smoothness for each participant was estimated and used for determining the threshold of cluster size in the group-level analysis. Motion correction was achieved based on censoring excessive motion (>0.2mm) from 12 motion parameters (3 rotational, 3 translational directions, and their 6 temporal derivatives). It is worth noting that the 0.2mm threshold is a relative stringent criterion as the comment thresholds are ranged from 0.2 to 0.5mm (9). Therefore, the regression step included 12 motion parameters and signals from eroded white matter and CSF masks. The residual time series after the preprocessing were used for all subsequent analyses.

Individual statistical maps were then calculated using a seed-based correlation analysis to infer the functional connectivity of the seed with the rest of the brain. The seed region of interest (ROI) was left M1 defined based on TMS site of SICI for each subject. A 10mm radius sphere was placed on each subject's structural images with individual SICI site as the center (Figure 3A). White matter and CSF were removed from the seed ROI using the masks obtained from FreeSurfer (10). Then, the mean time-series within seed ROI was correlated with the time course of each voxel in the brain for each subject. Pearson's correlation coefficients were converted to z values using Fisher's r-to-z transform.

DTI data preprocessing

The details of DTI data preprocessing were described in our previous studies (7, 11). DTI data was processed using the ENIGMA-DTI analysis pipeline (https://www.nitrc.org/projects/enigma_dti). All data included in the analysis passed the ENIGMA DTI quality assurance or quality control procedures. Specifically, a tract-based spatial statistics method was used for tract-based analysis of diffusion anisotropy (12). Raw images were corrected for motion and eddy currents using eddy correction tool distributed as a part of FMRIB Software Library (FSL) package version 5.0.9 (13). Fractional anisotropy (FA) images were created by fitting the diffusion tensor to the motion and eddy current corrected diffusion data. RMSDIFF (14) was used to estimate the root mean square movement distance between diffusion sensitized and b=0 images. All data passed QA control of<3 mm accumulated motion during the scan. All FA images were globally spatially normalized to the Johns Hopkins University (JHU) atlas (15) and then nonlinearly aligned to a group-wise, minimal-deformation target (MDT) brain using the FLIRT method (12). The group's MDT brain was identified by warping all individual brain images in the group to each other (13). The JHU atlas

was used to separate white matter into different tracts. Based on our previous findings that SICI deficit in schizophrenia can be largely explained by white matter microstructure of left corona radiata (CR) (7), but not the other 24 tracts in the whole brain, therefore, we included only left CR in the current study (Figure 3A). Some of the SICI and DTI data were reported in our previous work (5, 7). None of the resting-state fMRI or the fMRI/DTI/SICI cross-model analyses were previously reported.

Leave-one-out cross-validation (LOOCV)

We used LOOCV to evaluate the validities of obtained clusters (16). Specifically, clusters significantly associated with SICI or BPRS total score were iteratively re-estimated using the same thresholding procedures and N-1 participants. A significant cluster identified with full sample size has a high validity if it is replicated in more than 80% of the re-estimation with N-1 participants. For the 4 SICI-related clusters, all clusters except left cerebellum (50%) had high validities (92% for left middle prefrontal gyrus, 83% for right middle prefrontal gyrus, and 83% for right insula). For the 13 BPRS-related clusters, all clusters except left postcentral gyrus (50%) had high validities (88% - 100%). Thus, most clusters found here were under stringent correction and validation.

Supplemental Results and Discussion

Association between left PFC-M1 rsFC and motor retardation subscale

The left PFC-M1 rsFC was linked to both motor inhibition indexed by SICI and overall symptoms represented by BPRS total score in schizophrenia, suggesting this rsFC may play an important role in motor-related pathology of schizophrenia. Motor retardation is one of the motor dysfunctions

in schizophrenia and can be assessed by the item 13 in BPRS. Therefore, we evaluated whether this left PFC-M1 rsFC is also associated with this known motor deficit in schizophrenia by calculating the correlation between rsFC and motor retardation score in schizophrenia with age as a covariate. We found that higher rsFC was associated with less motor retardation (r=-0.47, p=0.02; Figure S3). This result confirmed the conclusion that left PFC-M1 rsFC was linked to motor deficits in schizophrenia. It further implied that the role of this rsFC in motor abnormalities may not be limited to motor inhibition.

Association between SICI and BPRS total score in schizophrenia

BPRS total score was positively related to SICI although it was not statistically significant in schizophrenia patients (r=0.26, p=0.23). Meanwhile, our findings show that left PFC-M1 rsFC was associated with both SICI and BPRS in patient group, suggesting there are shared neural underpinnings between motor inhibition at M1 and overall symptoms of schizophrenia. However, this doesn't necessarily imply there will be robust association between SICI and BPRS, as it is likely that the underlying circuitry for left PFC-M1 rsFC may support only some shared contributions to SICI and BPRS, but their individual variances are largely explained by other circuitries. For example, the rsFC between right insula and left M1 was only correlated with SICI, but not BPRS.

Difference of M1-seeded rsFC between healthy controls and schizophrenia patients

M1-seeded rsFC was compared between the two groups across the whole brain. Significant patient-control differences were observed at right insula (MNI: (46, 6, 4); t=4.63; cluster size: 645 voxels) and right Heschl's gyrus (MNI: (41, -29, 15); t=3.07; cluster size: 275 voxels) (Figure S4).

Left middle prefrontal cortex (MNI: (-23, 57, -1); t=4.23; cluster size: 111 voxels) separated patients from controls with a smaller cluster size (Figure S4). In all three clusters, healthy individuals had stronger rsFC than schizophrenia patients.

Reversed rsFC analysis was conducted using left middle prefrontal gyrus as seed

One advantage of the present study is using individualized TMS site to define individual M1 ROI for each participant. Further, to test whether the finding that left PFC-M1 was associated with SICI can be replicated using left PFC seed in the convention fixed ROI method, we conducted reversed rsFC analysis using left middle prefrontal gyrus as seed. We found the clusters showing significant correlation with SICI in schizophrenia included left PFC-M1 rsFC (Figure S5A). Similarly, the M1 cluster was also observed when testing the association between PFC-seeded rsFC and BPRS. Importantly, by overlapping the two significant cluster maps, we replicated our key finding that left PFC-M1 rsFC was significantly associated with both SICI and BPRS in schizophrenia (Figure S5B).

Association between left occipital cortex-seeded rsFC and SICI

Instead of using left M1 as seed, we used left occipital cortex as seed to calculate rsFC and re-run the same analysis pipeline to evaluate the association between rsFC and SICI. However, no significant correlation between left occipital cortex-seeded rsFC and SICI was observed. This suggests that the significant association between M1-PFC rsFC and SICI is not due to a diffused global effect of rsFC on SICI.

Table S1. Brain-behavioral correlations in healthy controls: significant brain areas whose resting state functional connectivity with left motor cortex were related with short-interval intracortical inhibition.

	Talairach (x, y, z) mm	Brodmann area	Cluster size	r
SICI related rsFC in healthy controls				
Left inferior parietal lobule	(-42, -33, 39)	40	164	-0.70*
Right middle frontal gyrus	(28, 28, 38)	8/9	292	0.80*
Right middle occipital gyrus	(50, -72, 8)	19/39	207	-0.70*

r: correlation coefficients between behavioral variables, i.e., Brief Psychiatric Rating Scale total score (BPRS Total) and short-interval intracortical inhibition (SICI), and the mean resting state functional connectivities (rsFCs) between motor cortex and each cluster. * corrected $p<0.05$.

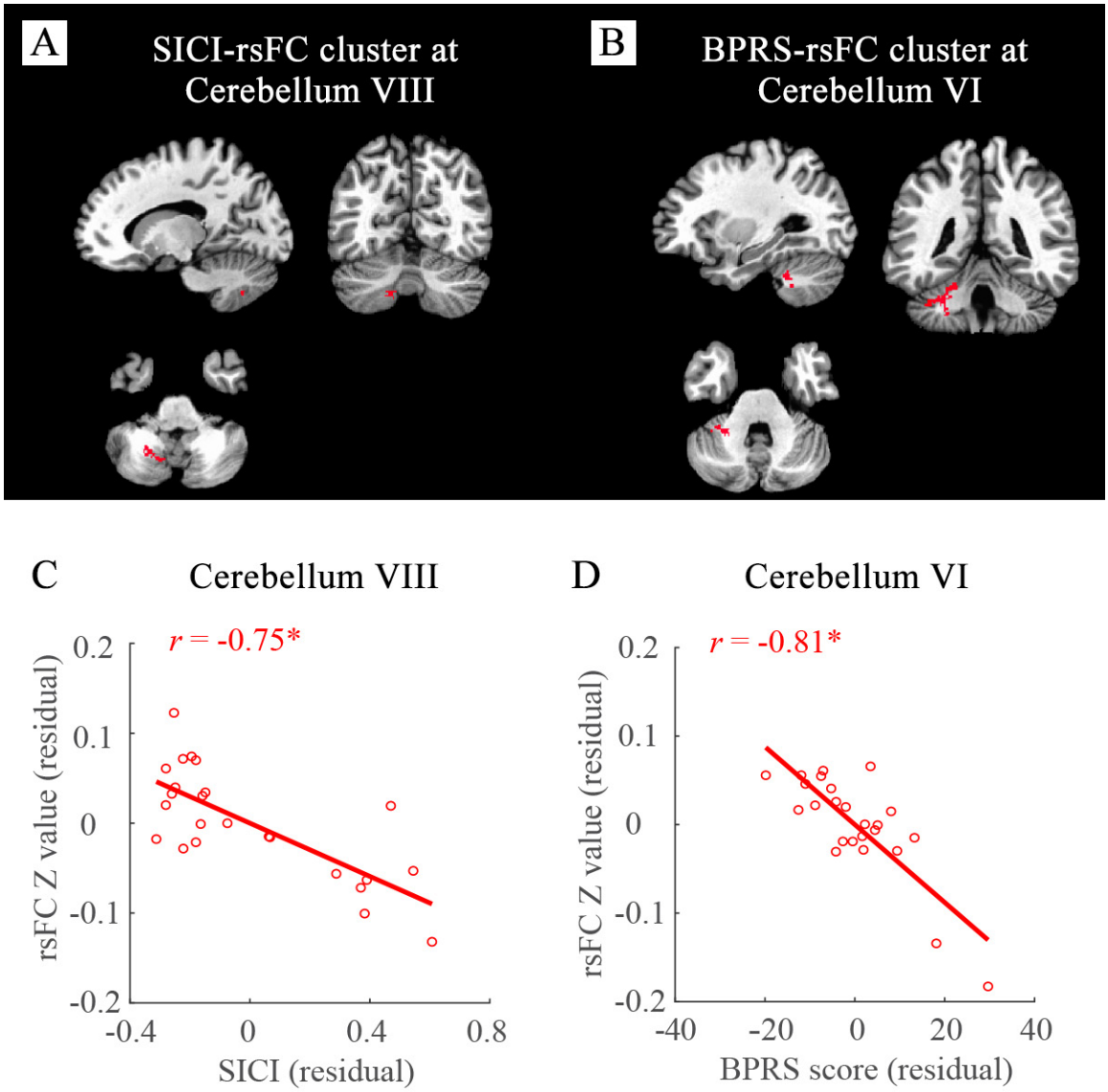

Figure S1. Association between left motor cortex (M1) resting state functional connectivity (rsFC) with subregions of cerebellum and short-interval intracortical inhibition (SICI) and symptoms of schizophrenia (BPRS). The M1 rsFC with cerebellum VIII (**A**) was associated with SICI (**C**). The higher the rsFC, the larger the cortical inhibition (i.e., smaller SICI). The M1 rsFC with cerebellum VI (**B**) was correlated with symptoms of schizophrenia (BPRS score) (**D**). The higher the rsFC, the less symptoms (smaller BPRS score). * corrected $p<0.05$.

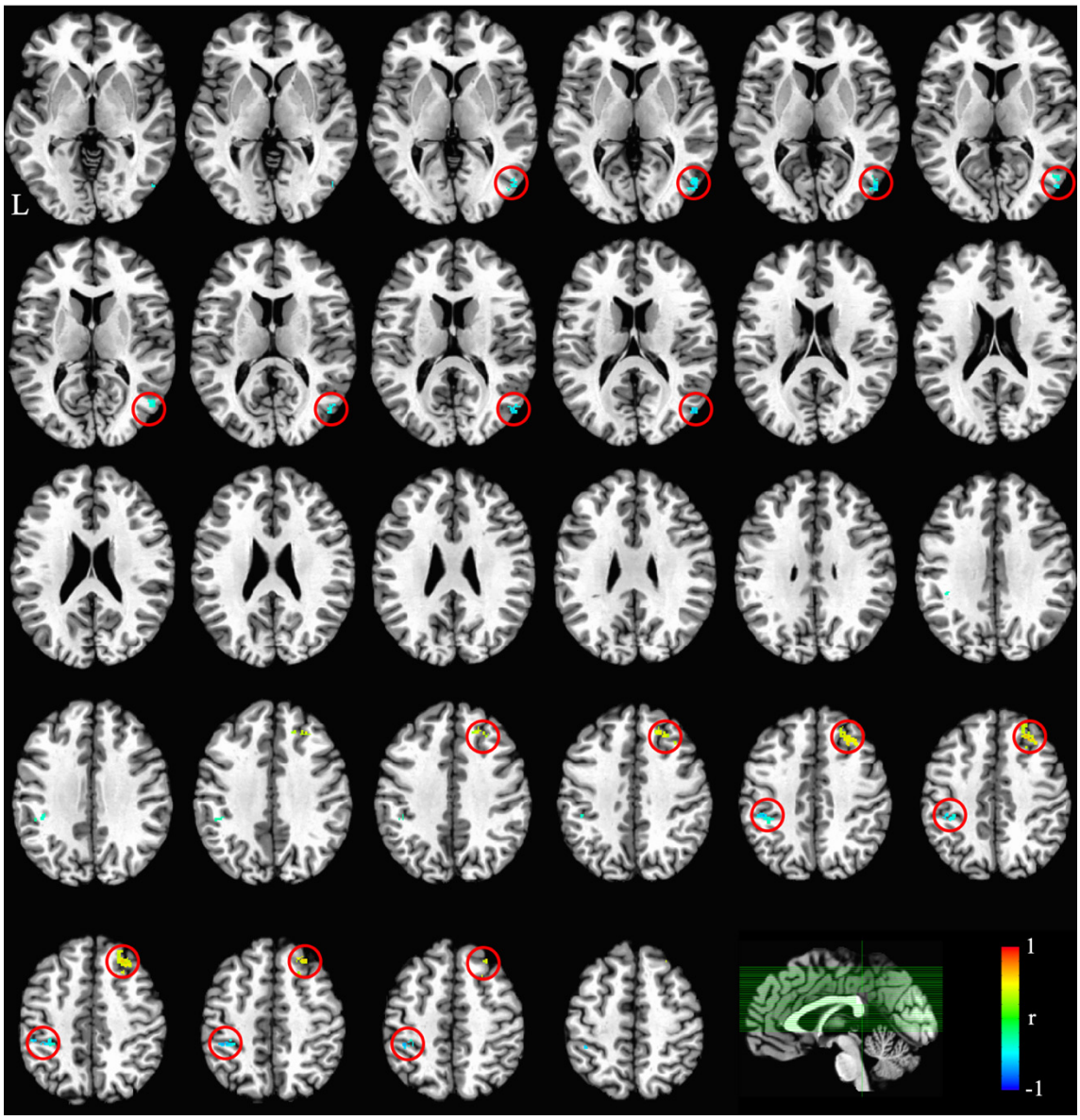

Figure S2. Significant associations between left M1-seeded resting state functional connectivity (rsFC) with short-interval intracortical inhibition (SICI) in healthy controls. Negative associations with SICI were mainly at left inferior parietal lobule and right middle occipital gyrus, while positive association was found at right middle frontal gyrus. Significant clusters were highlighted with purple circles (all corrected $p<0.05$).

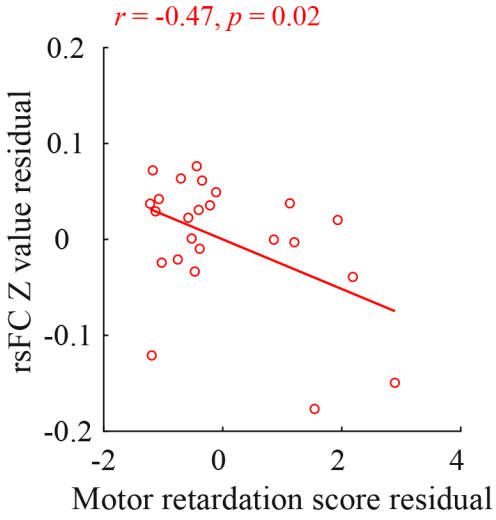

Figure S3. Significant associations between left M1-seeded rsFC at left middle prefrontal cortex with motor retardation in schizophrenia. Motor retardation score was obtained from the item 13 in Brief Psychiatric Rating Scale (BPRS). Higher rsFC at left middle prefrontal cortex was linked to less severe motor retardation.

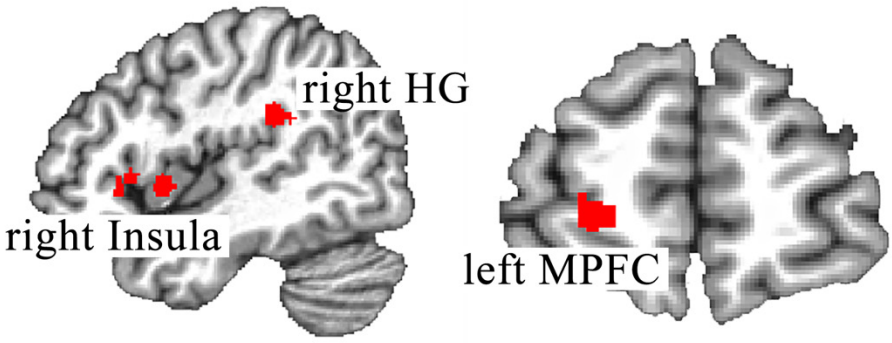

Figure S4. Left motor cortex-seeded resting-state functional connectivity (rsFC) showing differences between schizophrenia patients and healthy controls (see text above for statistics). HG, Heschl's gyrus. MPFC, middle prefrontal cortex. The rsFCs between left motor cortex and these clusters were smaller in schizophrenia patients than in healthy controls.

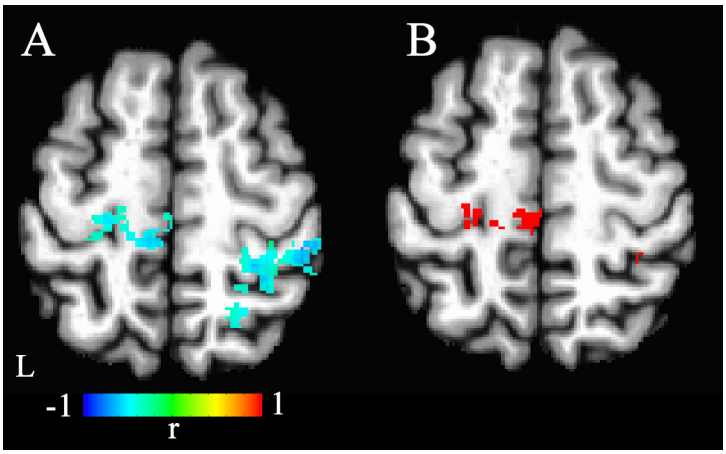

Figure S5. With left middle prefrontal gyrus (PFC) as the seed region, the left PFC-M1 resting state functional connectivity (rsFC) was still associated with short-interval intracortical inhibition (SICI) in schizophrenia (**A**). The conjunction areas whose rsFC with left middle PFC were associated with both SICI and total score of Brief Psychiatric Rating Scale (BPRS) included left PFC-M1 rsFC as well (**B**).

Supplemental References

1. Brasil-Neto JP, McShane LM, Fuhr P, Hallett M, Cohen LG (1992): Topographic mapping of the human motor cortex with magnetic stimulation: factors affecting accuracy and reproducibility. *Electroencephalogr Clin Neurophysiol*. 85:9-16.

2. Werhahn KJ, Fong JK, Meyer BU, Priori A, Rothwell JC, Day BL, et al. (1994): The effect of magnetic coil orientation on the latency of surface EMG and single motor unit responses in the first dorsal interosseous muscle. *Electroencephalogr Clin Neurophysiol*. 93:138-146.

3. Kammer T, Beck S, Thielscher A, Laubis-Herrmann U, Topka H (2001): Motor thresholds in humans: a transcranial magnetic stimulation study comparing different pulse waveforms, current directions and stimulator types. *Clin Neurophysiol*. 112:250-258.

4. Du X, Choa FS, Summerfelt A, Tagamets MA, Rowland LM, Kochunov P, et al. (2015): Neural summation in human motor cortex by subthreshold transcranial magnetic stimulations. *Exp Brain Res*. 233:671-677.

5. Du X, Summerfelt A, Chiappelli J, Holcomb HH, Hong LE (2014): Individualized brain inhibition and excitation profile in response to paired-pulse TMS. *J Mot Behav*. 46:39-48.

6. De Gennaro L, Marzano C, Veniero D, Moroni F, Fratello F, Curcio G, et al. (2007): Neurophysiological correlates of sleepiness: a combined TMS and EEG study. *NeuroImage*. 36:1277-1287.

7. Du X, Kochunov P, Summerfelt A, Chiappelli J, Choa FS, Hong LE (2017): The role of white matter microstructure in inhibitory deficits in patients with schizophrenia. *Brain Stimul*. 10:283-290.

8. Cox RW (1996): AFNI: software for analysis and visualization of functional magnetic resonance neuroimages. *Comput Biomed Res*. 29:162-173.

9. Power JD, Schlaggar BL, Petersen SE (2015): Recent progress and outstanding issues in motion correction in resting state fMRI. *NeuroImage*. 105:536-551.

10. Fischl B, Salat DH, Busa E, Albert M, Dieterich M, Haselgrove C, et al. (2002): Whole brain segmentation: automated labeling of neuroanatomical structures in the human brain. *Neuron*. 33:341-355.

11. Kochunov P, Coyle TR, Rowland LM, Jahanshad N, Thompson PM, Kelly S, et al. (2017): Association of White Matter With Core Cognitive Deficits in Patients With Schizophrenia. *JAMA Psychiatry*. 74:958-966.

12. Jones DK, Horsfield MA, Simmons A (1999): Optimal strategies for measuring diffusion in anisotropic systems by magnetic resonance imaging. *Magn Reson Med*. 42:515-525.

13. Smith SM, Jenkinson M, Johansen-Berg H, Rueckert D, Nichols TE, Mackay CE, et al. (2006): Tract-based spatial statistics: voxelwise analysis of multi-subject diffusion data. *NeuroImage*. 31:1487-1505.

14. Jahanshad N, Kochunov PV, Sprooten E, Mandl RC, Nichols TE, Almasy L, et al. (2013): Multi-site genetic analysis of diffusion images and voxelwise heritability analysis: a pilot project of the ENIGMA-DTI working group. *NeuroImage*. 81:455-469.

15. Smith SM, Jenkinson M, Woolrich MW, Beckmann CF, Behrens TE, Johansen-Berg H, et al. (2004): Advances in functional and structural MR image analysis and implementation as FSL. *NeuroImage*. 23 Suppl 1:S208-219.

16. Philip NS, Barredo J, van 't Wout-Frank M, Tyrka AR, Price LH, Carpenter LL (2018): Network Mechanisms of Clinical Response to Transcranial Magnetic Stimulation in Posttraumatic Stress Disorder and Major Depressive Disorder. *Biol Psychiatry*. 83:263-272.